Electronic Supplementary Material (ESI) for Lab on a Chip.

Supporting Information

A Disposable Microfluidic Device with a Reusable Magnetophoretic Functional Substrate for Isolation of Circulating Tumor Cells

Hyungseok Cho,[1] Jinho Kim,[1] Chang-Wan Jeon,[2] and Ki-Ho Han*,[1]

[1] Department of Nanoscience and Engineering
Center for Nano Manufacturing, Inje University
Gimhae 50834, Republic of Korea

[2] Department of Surgery
Gospel Hospital, Kosin University
Busan 49267, Republic of Korea

* E-mail: mems@inje.ac.kr

Tel: +82-55-320-3715/ Fax: +82-55-320-3631

S1. Instrument set-up

Two Nd-Fe-B permanent magnets were used and stacked for generating the external magnetic field for the assembly-disposable CTC-μChip. First, the reusable substrate was placed on the center of the two stacked permanent magnets to laterally apply the external magnetic field to the ferromagnetic wires. Then, the disposable polymeric superstrate was aligned to the ferromagnetic wire array and an air vacuum pressure of -50 kPa was applied for tight assembly with the reusable substrate. Three syringe pumps (Legato 100, KD Scientific) were used to control laminar flow in the microchannel. Two of them were used for injecting the blood sample and PBS buffer with 0.2% BSA at flow rates of 1–4 ml h^{-1}. Another was used to draw four-fifths of the solution flowing in the microchannel from the waste outlet, so the remaining one-fifth flowed into the CTC outlet.

S2. Theoretical analysis

According to a previous theoretical analysis,[1] the *x*-directional (horizontal) and *z*-directional (vertical) components of the magnetic force (F_m) acting on a CTC with a bound number N of magnetic nanobeads, beside location right above the rectangular wire, can be written as:

$$F_{mx} = -\frac{8NV_b M_b xka^2 B_0}{\pi\left(x^2+z^2\right)^2\sqrt{\left(x^2+z^2\right)^2+2k\left(\frac{w}{h}\right)a^2\left(x^2-z^2\right)+k^2\left(\frac{w}{h}\right)^2 a^4}}\left(\frac{w}{h}\right)\left[x^2-3z^2+k\left(\frac{w}{h}\right)a^2\right]$$

and [S1]

$$F_{mz} = -\frac{8NV_b M_b zka^2 B_0}{\pi\left(x^2+z^2\right)^2\sqrt{\left(x^2+z^2\right)^2+2k\left(\frac{w}{h}\right)a^2\left(x^2-z^2\right)+k^2\left(\frac{w}{h}\right)^2 a^4}}\left(\frac{w}{h}\right)\left[3x^2-z^2+k\left(\frac{w}{h}\right)a^2\right]$$

where $k = \frac{\mu_W - \mu_B}{\mu_W + \mu_B}$ [S2]

where V_b, and M_b are the volume and saturation magnetization field of the magnetic nanobead, respectively. The volume V_b and the saturation magnetization field M_b of the magnetic nanobeads used for analytical calculations and simulations are 6.54×10^{-23} m^3 and 30 kA/m, respectively. x and z represent the Cartesian coordinate with respect to the center of the ferromagnetic wire as the origin. B_0 (= 0.2 T) is the applied external magnetic flux. w (=70 μm) and h (= 40 μm) are the width and thickness of the rectangular ferromagnetic wire, respectively, and a can be replaced by $h/2$ as the effective radius of the rectangular wire. μ_B (= $4\pi\times10^{-7}$ H/m) and μ_W (= $800\,\mu_B$) are the permeabilities of the buffer solution and the ferromagnetic wire, respectively.

As shown in Fig. S2(a), the theoretical analysis revealed that the maximum *x*-directional magnetic force, F_{mx}, was ~1.3 nN based on the assumption that 100,000 magnetic nanobeads are bound on a single MCF7 cell, placed 17 μm height away from the wire. The force can be compared with the Stokes drag force (0.55−2.2 nN) on a MCF7 cell at flow rates of 1–4 ml h^{-1}. The theoretical analysis also revealed that the *x*-directional magnetic force increases as the thickness of polymer film is thinner, as expected. In addition to the *x*-directional magnetic force, F_{mx} (Eq. S1), there is a *z*-directional magnetic force, F_{mz} (Eq. S2) that pulls MCF7 cells toward the bottom of the microchannel. According to the theoretical analysis, as shown in Fig. S2(b), the maximum *z*-directional magnetic force on a MCF7 cell, bound to 100,000 magnetic nanobeads (50 nm in diameter) and placed 17 μm height away from the wires, is ~1.3 nN toward the bottom. Thus, as MCF7 cells approach the ferromagnetic wire, both horizontal and vertical magnetic forces increase simultaneously, followed by an increase in lateral displacement. Although some MCF7 cells pass over the forward ferromagnetic wires due to their initial levitation height, they are subsequently separated by the rearward ferromagnetic wires. Additionally, because the ferromagnetic wires are located at regular 300-

μm intervals in the reusable substrate, the lateral magnetic force is generated regularly over the entire area of the microchannel.

S3. RT-PCR protocol

To lyse the isolated CTCs, 100 μl of lysis/binding buffer (Dynabeads mRNA Direct Kit; Invitrogen Dynal AS) was added to the CTCs and mixed by pipetting. To extract mRNA, we used 2.8-μm-diameter magnetic beads (Dynabeads Oligo$(dT)_{25}$; Invitrogen Dynal AS) that bind oligo-dT sequences to their surface. Prior to mRNA extraction, a solution containing the oligo-dT magnetic beads was thoroughly suspended in a vial to obtain a uniform brown suspension. Then, 20 μl of the solution, as a suspension containing 3.7×10^3 beads μl^{-1}, was transferred to a 1.5-ml tube. The beads were washed twice with lysis/binding buffer. The wash solution was removed from the oligo-dT magnetic beads, and the CTC lysate was added to the tube. The sample solution was then mixed with a pipette for 5 min at room temperature to allow mRNA to bind to the oligo-dT beads. The tube was then placed on a magnet for 2 min to collect the oligo-dT magnetic beads, and the supernatant was removed. Oligo-dT beads and mRNA complex were washed and resuspended in 300 μl of washing buffer A (Dynabeads mRNA Direct Kit) at room temperature. The magnet was used to separate the oligo-dT beads from the solution. The oligo-dT beads and mRNA complex were washed twice more using 300 μl of washing buffer B (Dynabeads mRNA Direct Kit). The tube was placed on the magnet, washing buffer B was removed, and cDNA reagents were added to the oligo-dT beads with bound mRNA.

For the cDNA synthesis, AccuPower CycleScript RT PreMix (dT20) (Bioneer) was used and dissolved using 20 μl of 0.1% diethylpyrocarbonate (DEPC)-treated water. After adding the mRNA template into the dissolved solution, the reaction mixture was incubated at 37°C for

30 s, 48°C for 4 min, and 55°C for 30 s for 12 cycles and RNase inactivation step at 95°C for 5 min, in sequence.

The epithelial-originated CTC-specific gene (keratin 19; KRT19, 211 bp)[2] was amplified with forward and reverse primers (5'-TTTGAGACGGAACAGGCTCT-3' and 5'-AATCCACCTCCACACTGACC-3'). The epithelial cell adhesion molecule gene (EpCAM, 287 bp)[3] was amplified (using 5'-GCGTTCGGGCTTCTGCTTGC-3' and 5'-CCGCTCTCATCGCAGTCAGGA-3'). A human housekeeping gene (β-actin, 244 bp) was amplified as a positive control (using the primers 5'-GTACCACTGGCATCGTGATGGA-3' and 5'-GCCATCTCTTGCTCGAAGTCCAG-3'). The 20-μl PCR mixture was prepared in a 200-μl tube containing PCR reagent powder (AccuPower HotStart PCR PreMix; Bioneer), 1 μl of forward and reverse primers (10 pmol μl^{-1}), 3 μl of cDNA template, and 16 μl of 0.1% DEPC water. Using a commercial thermocycler (GeneAmp PCR System 9700; Applied Biosystems), PCR thermocycling conditions for β-actin and KRT19 consisted of 1 cycle of denaturing at 95°C for 10 min, 40 cycles of 94°C for 30 s, 55°C for 30 s, and 72°C for 30 s, followed by a final extension at 72°C for 10 min. Thermocycling conditions for EpCAM were as follows: denaturation at 95°C for 10 min, 50 cycles of 95°C for 45 s, 63°C for 45 s, and 72°C for 30 s, followed by a final extension at 72°C for 10 min. PCR products were analyzed by 2% agarose (Invitrogen) gel electrophoresis with ethidium bromide (Promega) staining, followed by observation under UV light to compare the product sizes based on fluorescently labeled DNA standards.

REFERENCES

(1) Kim, S.; Han, S.-I.; Park, M.-J.; Jeon, C.-W.; Joo, Y.-D.; Choi, I.-H.; Han, K.-H. *Analytical Chemistry* **2013**, *85*, 2779-2786.

(2) Tanaka, F.; Yoneda, K.; Hasegawa, S. *Lung Cancer: Targets and Therapy* **2010**, *1*, 77-84.

(3) Wong, N. A.; Warren, B. F.; Piris, J.; Maynard, N.; Marshall, R.; Bodmer, W. F. *J Clin Pathol* **2006**, *59*, 260-263.

Table S1. A statistical comparative analysis of the bond strengths of the silicone-coated release PET film and PDMS linker-coated PET film to the PDMS. The t-value of the bond strengths of the two groups was caluated as 1.179. For 95% confidance interval and 9 degree of freedom, the critical value for the t-distribution is 2.262, which is larger than the t-value. Thus, the difference between the bond strengths of the two groups is not meaningful.

Type	Number of samples	Mean [kPa]	Standard deviation [kPa]	t-value
Silicone-coated release PET film	10	617	106	1.179
PDMS linker-coated PET film	10	514	255	

Table S2. Summary of circulating tumor cell counts from 5-ml blood samples from healthy donors (n = 2) and patients with breast cancer (n = 20), as presented in Fig. 6(b).

Sample ID	Cancer type	Age	Stage	Treatment	CTC count	EpCAM	KRT19
H1	Healthy donor	44			0	⊘	⊘
H2	Healthy donor	49			0	⊘	⊘
P1	Invasive ductal carcinoma breast cancer	43	I	Naïve Pre-operation	6	○	⊘
P2	Invasive ductal carcinoma breast cancer	51	I	Naïve Pre-operation	6	○	⊘
P3	Invasive ductal carcinoma breast cancer	44	I	Naïve Pre-operation	7	○	⊘
P4	Invasive ductal carcinoma breast cancer	44	I	Naïve Pre-operation	21	○	⊘
P5	Invasive ductal carcinoma breast cancer	80	I	Naïve Pre-operation	31	○	○
P6	Invasive ductal carcinoma breast cancer	47	II	Naïve Pre-operation	3	○	⊘
P7	Invasive ductal carcinoma breast cancer	57	II	Naïve Pre-operation	9	⊘	⊘
P8	Invasive ductal carcinoma breast cancer	47	II	Naïve Pre-operation	20	⊘	⊘
P9	Invasive ductal carcinoma breast cancer	57	II	Naïve Pre-operation	29	⊘	⊘
P10	Invasive ductal carcinoma breast cancer	53	II	Naïve Pre-operation	33	No Data	⊘
P11	Invasive ductal carcinoma breast cancer	49	II	Naïve Pre-operation	70	⊘	⊘
P12	Invasive ductal carcinoma breast cancer	67	III	Naïve Pre-operation	22	⊘	○
P13	Invasive ductal carcinoma breast cancer	58	III	Naïve Pre-operation	36	○	○
P14	Invasive ductal carcinoma breast cancer	67	III	Naïve Pre-operation	61	○	⊘
P15	Invasive ductal carcinoma breast cancer	66	III	Naïve Pre-operation	88	⊘	⊘
P16	Invasive ductal carcinoma breast cancer	68	IV	Naïve Pre-operation	42	○	○
P17	Invasive ductal carcinoma breast cancer	61	IV	Naïve Pre-operation	80	○	⊘
P18	Invasive ductal carcinoma breast cancer	72	IV	Naïve Pre-operation	92	○	○
P19	Invasive ductal carcinoma breast cancer	64	II	Chemotherapy	9	○	⊘
P20	Invasive ductal carcinoma breast cancer	45	II	Post-operation	0	⊘	⊘

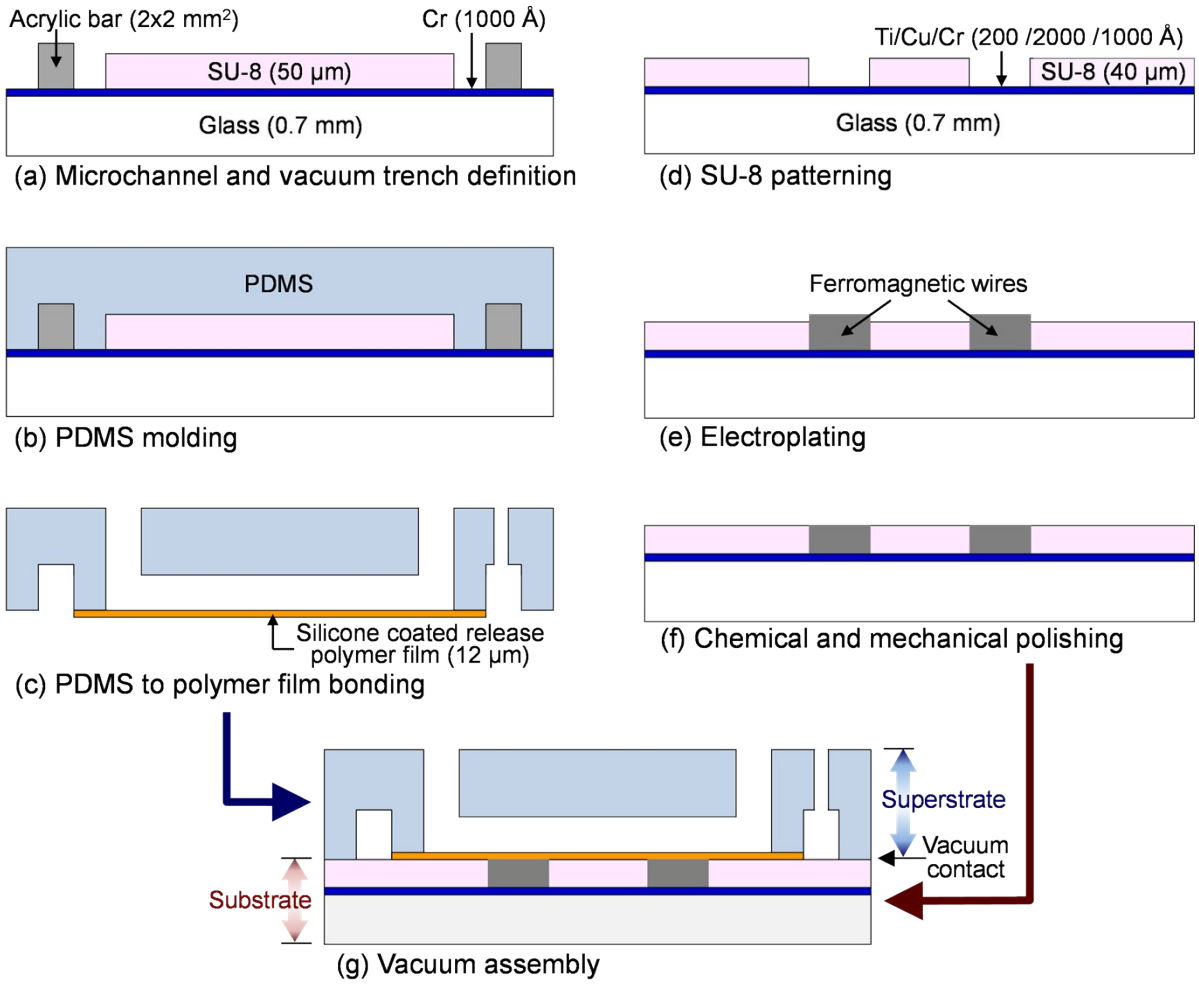

Fig. S1 Fabrication process for the assembly-disposable CTC-μChip. (a) Cr (1000 Å) deposition on a glass slide, SU-8 patterning to define the microchannel, and the acrylic square bar (2 × 2 mm^2) adhesive bonding to define the vacuum trench. (b) PDMS molding to make the microstructured PDMS replica. (c) Inlets, outlets, and vacuum hole were created with a 1.5-mm diameter punch and oxygen plasma bonding of the PDMS replica and the silicone-coated release 12-μm-thick PET film, producing the disposable polymeric superstrate. (d) Ti/Cu/Cr (200/2000/1000 Å) deposition on a glass substrate and SU-8 patterning to make the 40-μm-thick micromold. (e) Permalloy ($Ni_{0.8}Fe_{0.2}$) electroplating of the ferromagnetic wires. (f) Chemical and mechanical permalloy polishing to create the inlaid ferromagnetic wire array, completing fabrication of the reusable substrate. (g) Vacuum assembly of the disposable polymeric superstrate and the reusable substrate to build the assembly-disposable CTC-μChip.

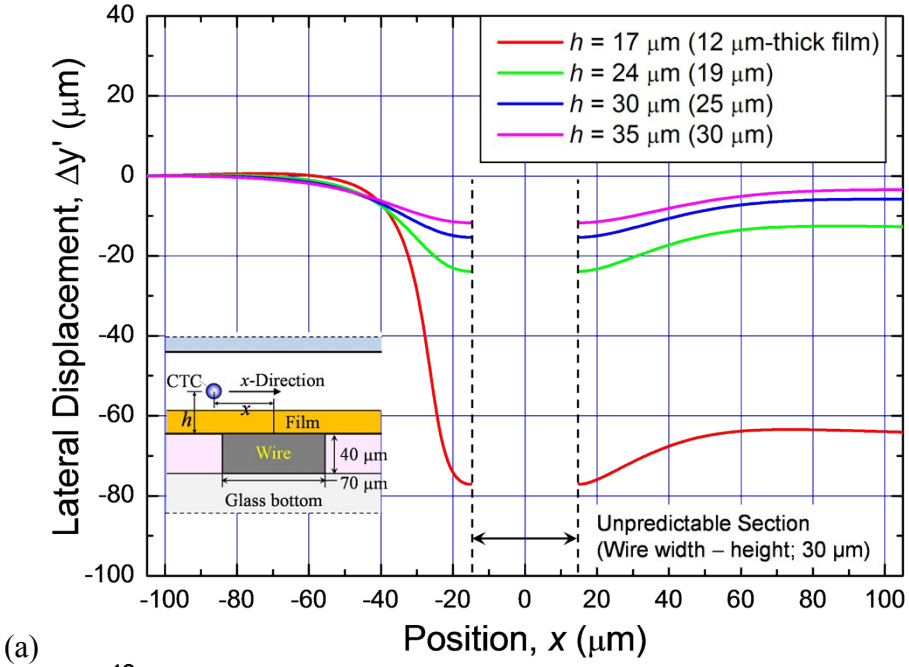

(a)

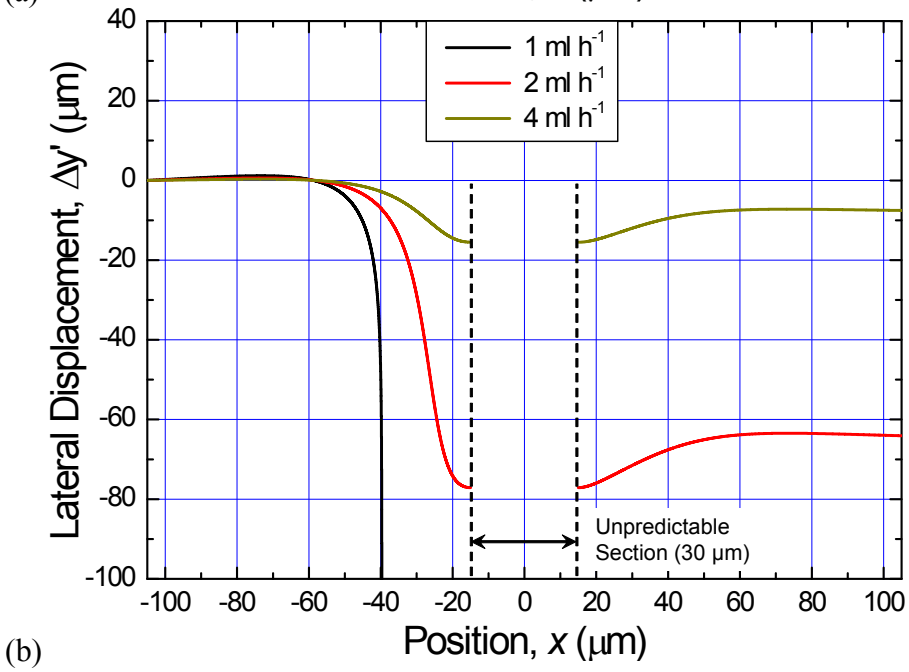

(b)

Fig. S2. Analytical results of the lateral displacement, Δy', of a CTC (bound with magnetic nanobeads) passing over a single rectangular ferromagnetic wire (70 × 40 μm^2) at (a) a flow rate of 2 ml h^{-1} with various thickness (12, 19, 25 and 30 μm) of PET film and (b) various flow rates (1, 2 and 4 ml h^{-1}) with a 12-μm-thick PET film. Then, it was assumed that the CTC (10 μm in diameter) is flowing on the bottom surface of the microchannel and bound with 4,000 magnetic nanobeads (50 nm in diameter). The external magnetic flux is 0.2 T. The gray rectangle in the inset represents the cross-section of the rectangular ferromagnetic wire, taken perpendicular to the *x*-axis in Fig. 1(c).

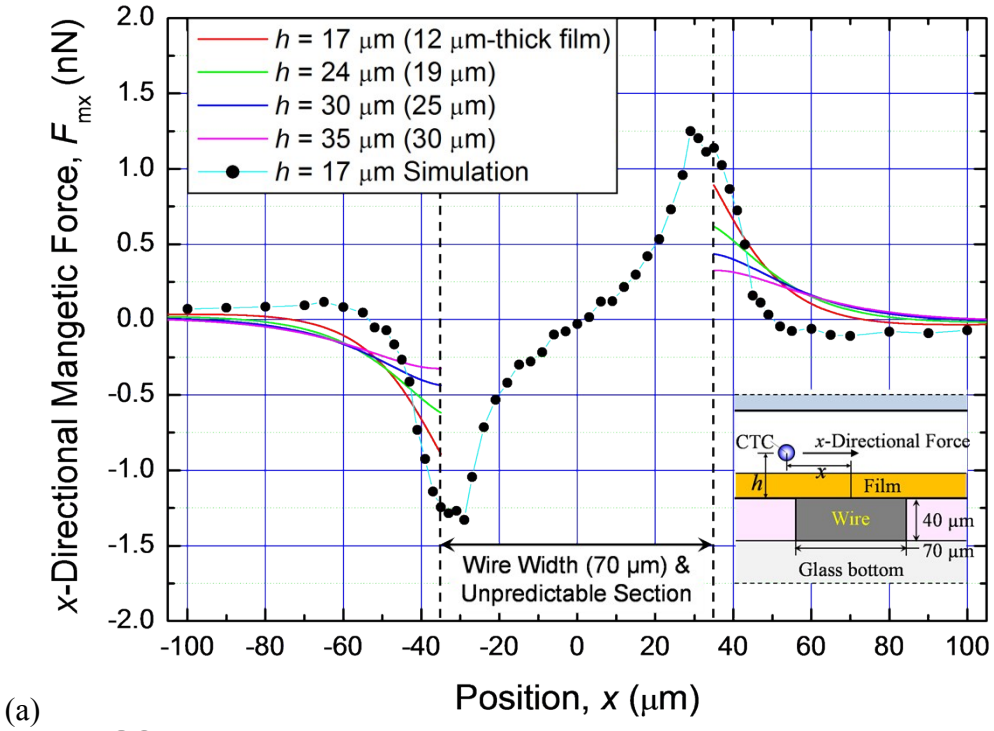

(a)

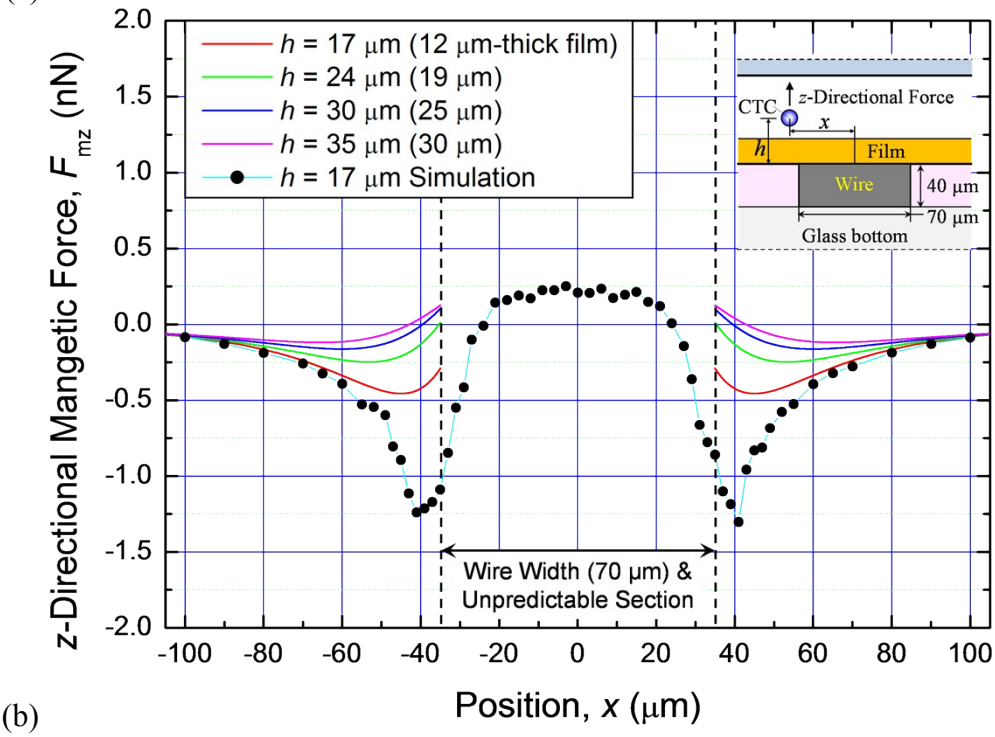

(b)

Fig. S3. Calculated and simulated (a) *x*- and (b) *z*-directional magnetic forces acting on a CTC located at various heights, h, and bound with 100,000 magnetic nanobeads (50 nm in diameter) in an external magnetic flux of 0.2 T. The gray rectangle in the inset represents the cross section of the rectangular ferromagnetic wire (70 × 40 μm^2), taken perpendicular to the *x*-axis in Fig. 1(c).

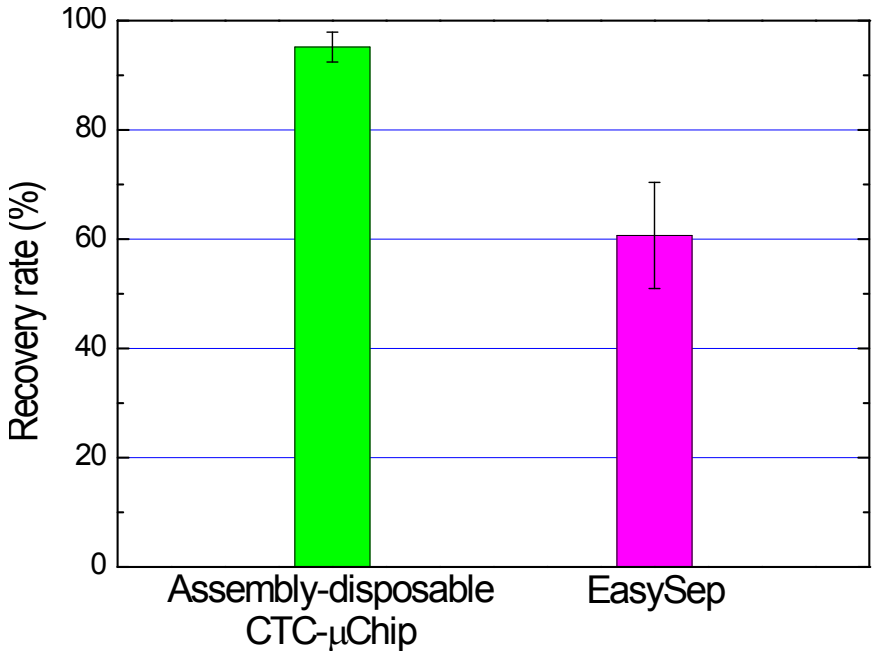
Recovery rate (%)
100
80
60
40
20
0
Assembly-disposable CTC-μChip
EasySep

(a)

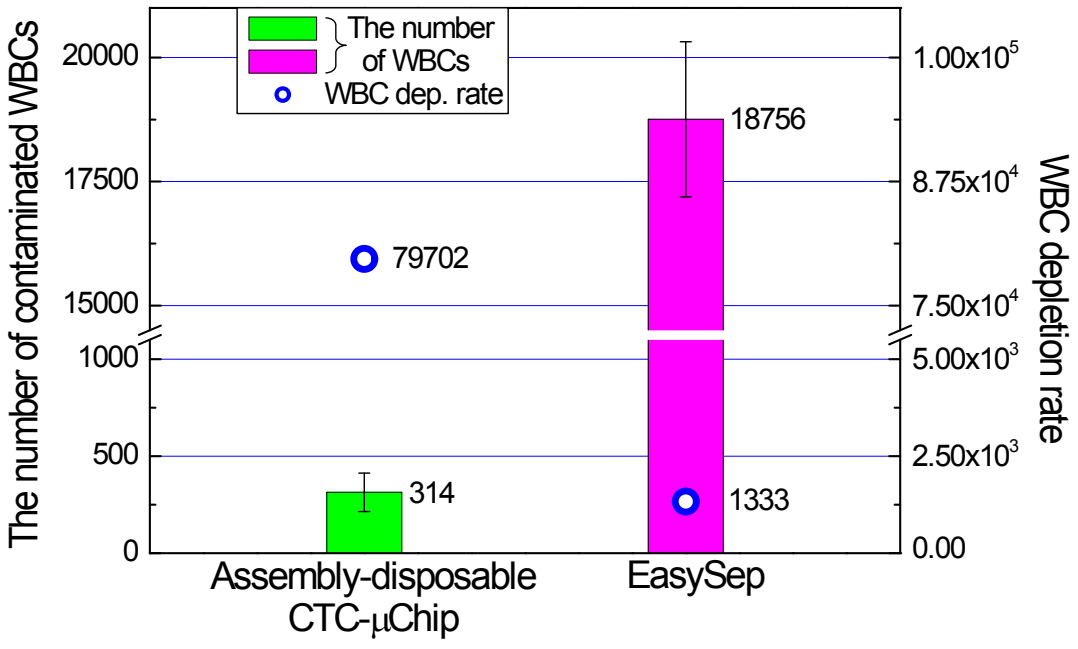
The number of contaminated WBCs
20000
17500
15000
1000
500
0
The number of WBCs
WBC dep. rate
79702
314
18756
1333
1.00x10^5
8.75x10^4
7.50x10^4
5.00x10^3
2.50x10^3
0.00
WBC depletion rate
Assembly-disposable CTC-μChip
EasySep

(b)

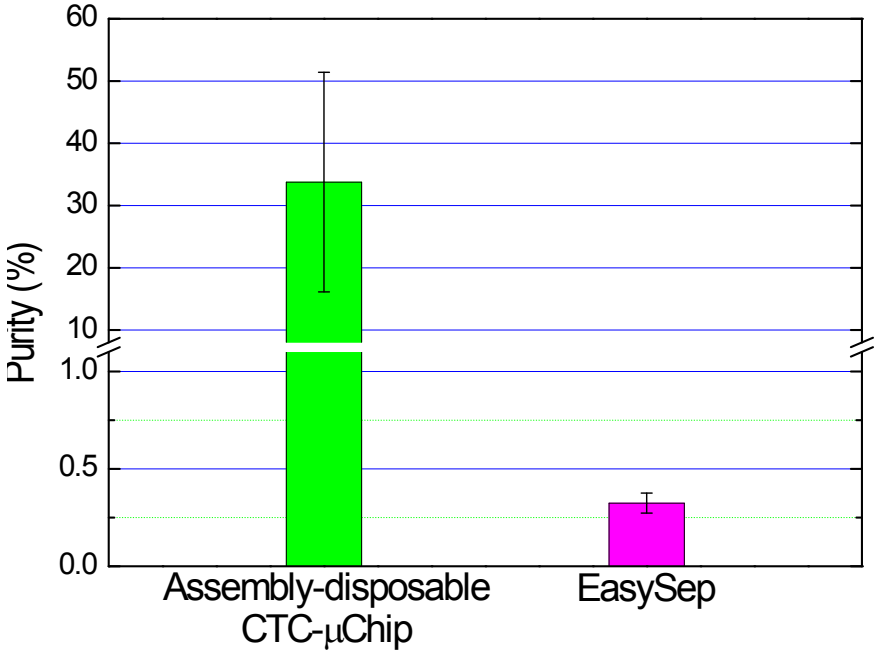

(c)

Fig. S4 (a) Recovery rates of MCF7 cells, (b) the number of contaminating WBCs and (c) the purities of isolated MCF7 cells, isolated using the assembly-disposable CTC-μChip with 12-μm-thick PET film at a flow rate of 2 ml h^{-1} and EasySep Human EpCAM Positive Selection Kit (STEMCELL Technologies). For the experiment, nucleated blood cells, prepared by Ficoll density gradient centrifugation of peripheral blood (5 ml) spiked with breast cancer cell lines (~100 MCF7 cells), were used. The error bars represent one standard deviation of three measured datasets.

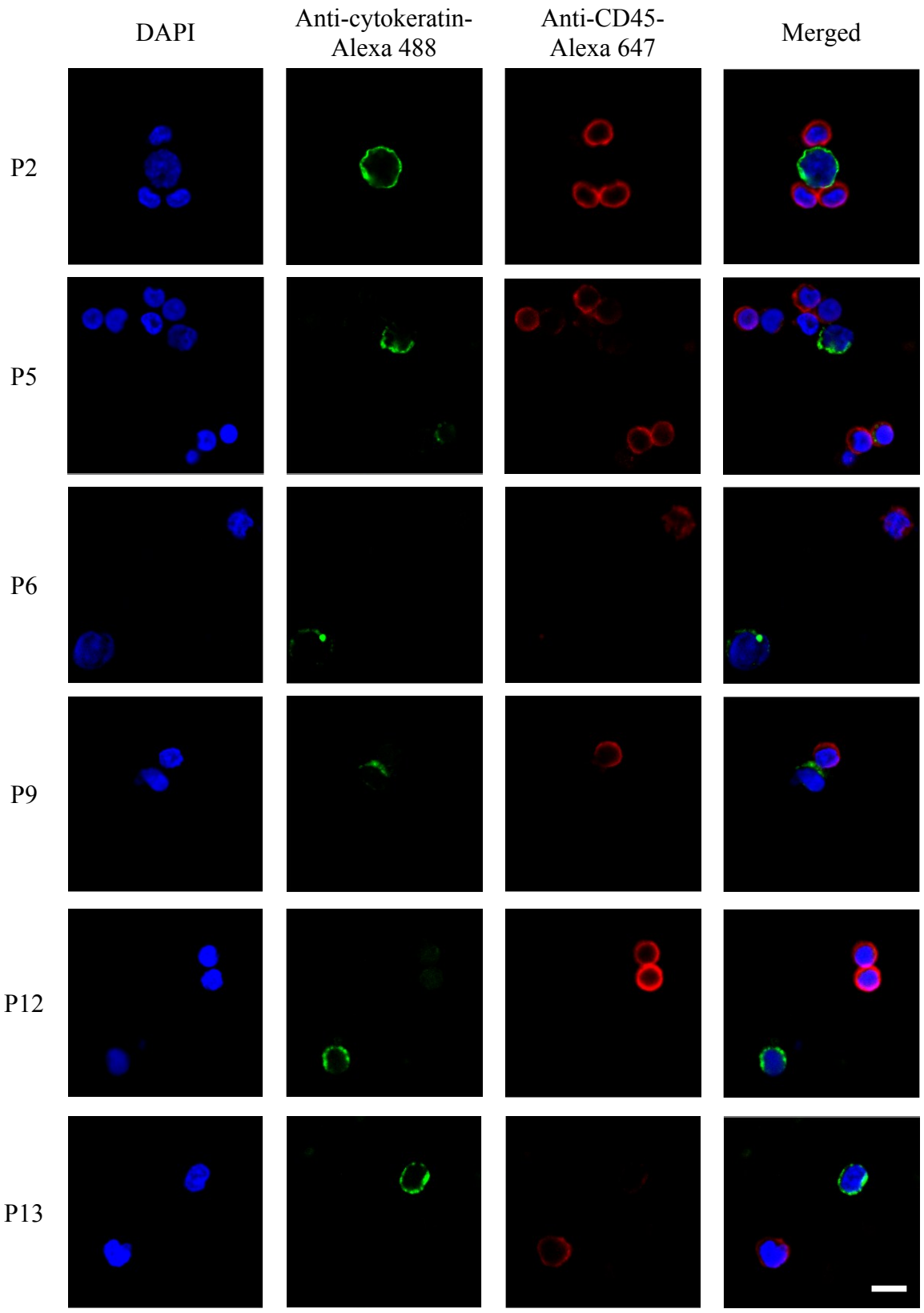

Fig. S5. Photomicrographs of breast CTCs stained using the immunofluorescent dyes DAPI, anti-cytokeratin-Alexa 488, and anti-CD45-Alexa 647. The scale bar represents 10 μm.